

## ARTICLES

**Boolean and Fuzzy Logic Gates Based on the Interaction of Flindersine with Bovine Serum Albumin and Tryptophan**

Pier Luigi Gentili\*

*Dipartimento di Chimica, Università di Perugia, 06123 Perugia, Italy**Received: July 30, 2008; Revised Manuscript Received: September 22, 2008*

The naturally occurring photochromic compound, flindersine (FL), interplays with bovine serum albumin (BSA) and tryptophan (Trp). The intermolecular forces that establish between the couples FL/BSA and FL/Trp exert mutual effects on their photobehavior. These reciprocal effects can be exploited, in the field of molecular computing, to implement specific binary logic gates based on chemical inputs, physical outputs, and UV photons as power supply. Moreover, the smooth dependence of BSA and Trp fluorescence quantum yields on addition of FL moles ( $n_{FL}$ ) and temperature ( $T$ ), allows us to process fuzzy logic. The synergistic action of the two inputs ( $n_{FL}$  and  $T$ ) allows the fuzzy AND logic gate to be implemented.

**1. Introduction**

In recent years, there have been significant efforts made in exploring the possibilities of molecular computing.<sup>1–3</sup> The ultimate goal is to build a computer, similar in its basic operation to current silicon-based machines, with its underlying hardware based on single molecules, supramolecular entities, and/or chemical reaction networks.

If chemical computers want to fulfill every need of computing, then it is compelling to find out how to implement not only Boolean logic gates but also fuzzy logic. Boolean binary logic has the peculiarity of manipulating only statements that are true or false, reducible to strings of zeros and ones. However, quite often, the available data and knowledge suffer a certain degree of uncertainty and imprecision, especially when they are based on subjective linguistic statements. In all of these cases, it is still possible to process information by abandoning hard computing, based on binary logic and crisp systems, and adopting soft computing, based on fuzzy logic, neural nets, and probabilistic reasoning.<sup>4</sup> Fuzzy logic is likely to play an increasingly important role in the conception and design of systems whose machine intelligence quotient is much higher than that of systems designed by conventional methods, since it would be able to deal with certain and uncertain information, objective and subjective knowledge. The most effective implementations of fuzzy logic in electronics have been achieved by the use of analog electronic circuits that are based on continuously variable signals. At the molecular level, it has been demonstrated that fuzzy logic can be processed through the DNA hybridization reaction<sup>5</sup> and the fuzzy AND logic gate can be implemented through the proximity effect exhibited by the electronic excited states of aromatic carbonyl and nitrogen-heterocyclic compounds.<sup>6</sup>

In this work, it is shown how it is possible to implement simple Boolean and fuzzy logic gates by exploiting the intermolecular forces that a naturally occurring photochromic

compound, flindersine (FL), establishes with a protein, bovine serum albumin (BSA), and the amino acid tryptophan (Trp).

**2. Materials and Methods.** For the description of the materials and experimental methods adopted to characterize the photophysics of bovine serum albumin (BSA), tryptophan (Trp), and flindersine (FL) and the photochromic behavior of FL, see ref 7. To build up Fuzzy Logic Engines based on the Mamdani's and Sugeno's methods, the Fuzzy Logic Toolbox for Use with MathLab<sup>8</sup> has been employed.

**3. Results and Discussion**

**3.1. Boolean Logic Gates.** BSA and Trp are fluorescent compounds whose emission bands fall over an absorption band of FL. Therefore, their spectral properties are ideal for having efficient resonance energy transfer from the protein or the amino acid to FL. Some experiments, described in ref 7 confirm the expectations. FL interacts strongly with BSA, determining both static and dynamic quenching of the fluorescence of the macromolecule. This means that both the fluorescence quantum yield and excited-state lifetime of BSA are reduced by addition of FL. Alternatively, fluorescence anisotropy of BSA is insensitive to the presence of FL. These evidence allow some Boolean logic gates to be defined. The input is, in every case, the ratio of FL to BSA moles ( $n_{FL}/n_{BSA}$ ); the outputs are the fluorescence quantum yield ( $\Phi_F(BSA)$ ), lifetime ( $\tau_{BSA}$ ) and anisotropy ( $r_{BSA}$ ) of BSA. UV photons (having  $\lambda_{exc}=275$  nm) constitute the power supply of the macromolecular processor. If positive logic conventions are adopted for all the variables involved and the threshold values of 20 for the ratio  $n_{FL}/n_{BSA}$ , 0.04 for  $\Phi_F(BSA)$ , 4.8 ns for  $\tau_{BSA}$ , and 0.15 for  $r_{BSA}$  (associated to a threshold value for the input  $n_{FL}/n_{BSA} = 5$ ) are fixed, then two NOT and one PASS 0 logic gates can be implemented (see Figure 1 and Table 1), based on  $\Phi_F(BSA)$ ,  $\tau_{BSA}$  and  $r_{BSA}$ , respectively. On the basis of luminescence relaxation times, their speed of computation is on the order of gigahertz.

The interplay between BSA and FL brings about effects not only on the photophysics of the macromolecular host species, but also on the photoresponse of the guest molecules. In fact,

\* To whom correspondence should be addressed. Tel: +39 075 5855576. Fax: +39 075 5855598. E-mail: pierluigi.gentili@unipg.it.

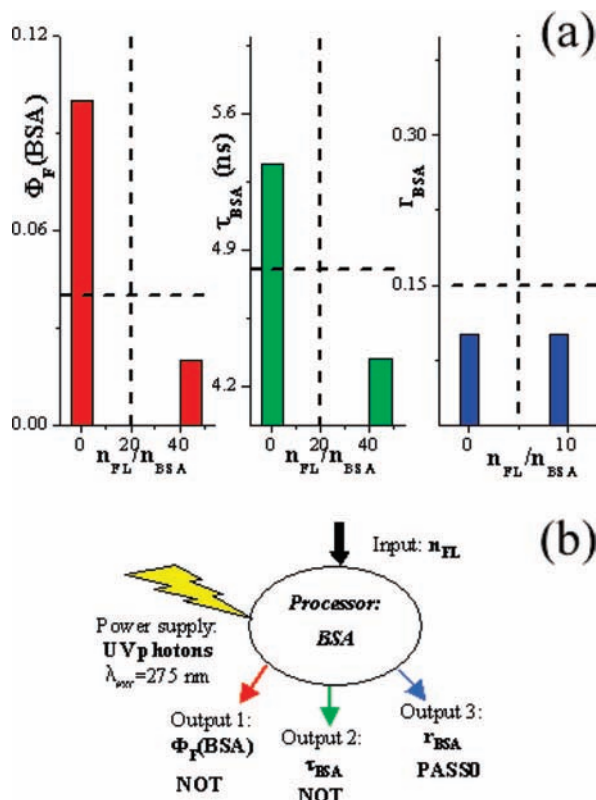
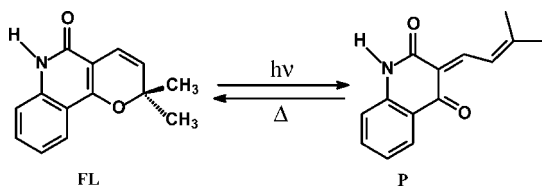


**Figure 1.** (a) Bar representation of the three logic gates based on the emission properties of BSA. The vertical and horizontal dashed segments represent the threshold values for the variables involved. (b) Representation of the Boolean logic functions that can be processed by exploiting the sensitivity of the BSA emission to FL molecules.

**TABLE 1: Truth Tables of the NOT and PASS 0 Logic Elements Based on the Emission Properties of BSA Sensitive to the Presence of FL**

INPUT	OUTPUTS		
$n_{FL}/n_{BSA}$	$\Phi_F(BSA)$	$\tau_{BSA}$	$\Gamma_{BSA}$
0 (low)	1 (high) > 0.04	1 (long) > 4.8 ns	0 (low) < 0.15
1 (high)	0 (low) < 0.04	0 (short) < 4.8 ns	0 (low) < 0.15
	NOT	NOT	PASS 0

**SCHEME 1: Photo-electrocyclization and Thermal Back Reaction of FL**



the microenvironment created by the protein prolongs the fluorescence lifetime ( $\tau_{FL}$ ) of FL and makes it a brighter species (i.e., the fluorescence quantum yield of FL,  $\Phi_F(FL)$ , grows up). Moreover, BSA acts as a catalyst toward the photoreaction of FL, determining an increase of the reaction quantum yield ( $\Phi_{PC}(FL)$ , see Scheme 1 for a sketch of FL photochemistry; the conversion of FL to P determines a reduction of absorbance in the spectral region included between 343 and 375 nm and an absorbance increase between 300 and 333 nm).<sup>7</sup>

This phenomenology can be exploited to implement further Boolean logic gates, wherein the ratio of BSA to FL moles,  $n_{BSA}/n_{FL}$ , is the input and the fluorescence quantum yield, emission lifetime, and reaction quantum yield of FL are the

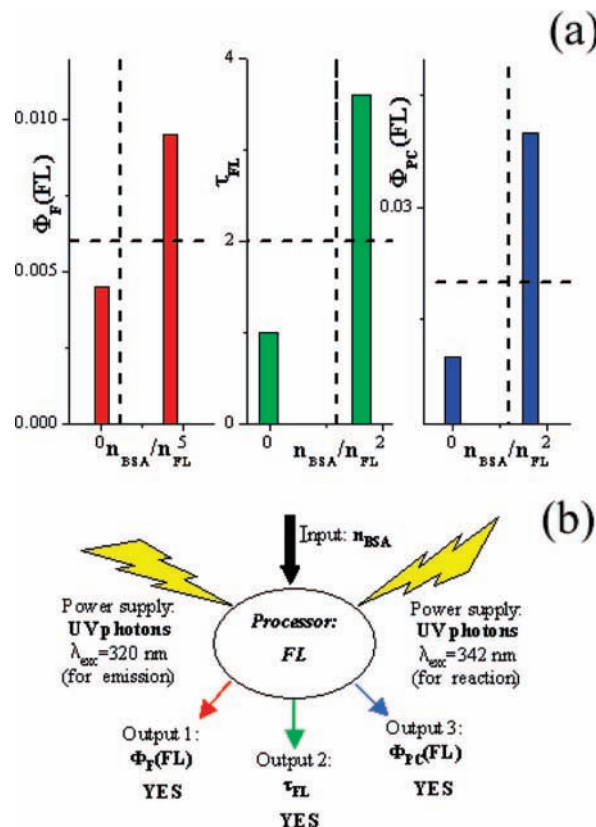


**Figure 2.** (a) Bar representation of the three logic gates that are based on the photoresponse of FL in the presence or absence of BSA. The vertical and horizontal dashed segments represent the threshold values for the variables involved. (b) Representation of the Boolean logic functions that can be processed by exploiting the sensitivity to BSA of FL photoresponse.

**TABLE 2: Truth Tables of the YES Logic Elements Based on the FL Photo-Behavior, Sensitive to BSA**

INPUT	OUTPUTS		
$n_{BSA}/n_{FL}$	$\Phi_F(FL)$	$\tau_{FL}$	$\Phi_{PC}(FL)$
0 (low) < 1.2	0 (low) < 0.006	0 (short) < 2 ns	0 (low) < 0.02
1 (high) > 1.2	1 (high) > 0.006	1 (long) > 2 ns	1 (high) > 0.02
	YES	YES	YES

outputs. If positive logic conventions are adopted for all the variables involved and the threshold values of 1.2 for the ratio  $n_{BSA}/n_{FL}$ , 0.006 for  $\Phi_F(FL)$ , 2 ns for  $\tau_{FL}$ , and 0.02 for  $\Phi_{PC}(FL)$  are fixed, then three different YES logic gates can be implemented, with UV photons as energy supply. They are portrayed in Figure 2 and summarized in Table 2. The speed of computation for the gates based on the FL luminescence is high, since they reset with a frequency of the order of gigahertz; rather slower is the reset time for the logic operation YES defined through the photoelectrocyclization reaction of FL, since the thermal back reaction requires roughly 40 min.

The spectral overlapping of the emission band of Trp with an absorption band of FL, similar to what comes about with BSA, hints that energy transfer from the amino acid to FL can also occur. This is confirmed by the effective quenching of Trp fluorescence by FL. The quenching mechanism has static and not dynamic character since the excited-state lifetime of Trp is unaffected by the addition of the photochromic compound. The action of FL molecules toward the emission properties of Trp can be exploited to define further Boolean logic gates. If the ratio of FL to Trp moles ( $n_{FL}/n_{Trp}$ ) is employed as input, UV photons of 275 nm as power supply, and Trp fluorescence

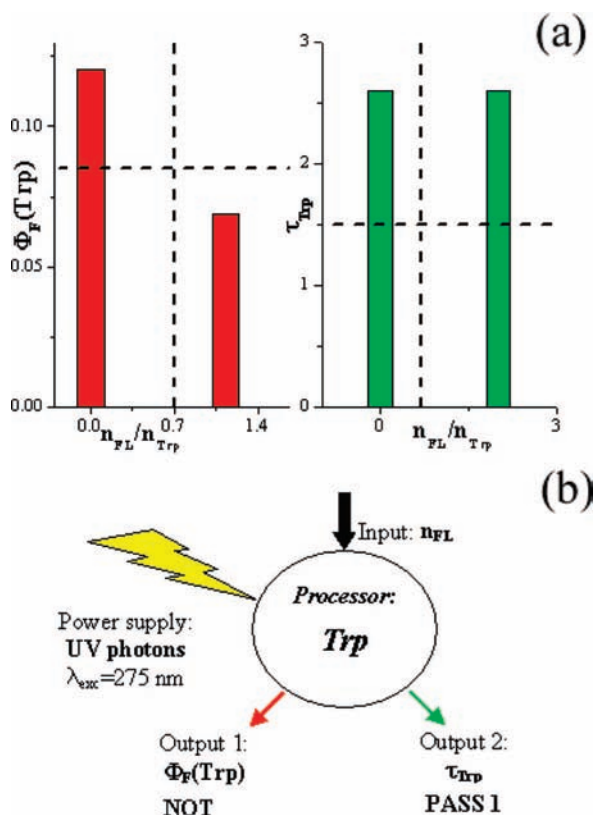


**Figure 3.** (a) Bar representation of the two logic gates, NOT and PASS 1, based on the emission properties of Trp. The vertical and horizontal dashed segments represent the threshold values for the variables involved. (b) Representation of the Boolean logic functions that can be processed by exploiting the sensitivity of the Trp emission toward FL molecules.

**TABLE 3: Truth Tables of the NOT and PASS1 Logic Elements**

INPUT	OUTPUTS	
$n_{\text{FL}}/n_{\text{Trp}}$	$\Phi_F(\text{Trp})$	$\tau_{\text{Trp}}$
0 (low) < 0.7	1 (high) > 0.08	1 (long) > 1.5 ns
1 (high) > 0.7	0 (low) < 0.08	1 (long) > 1.5 ns
	<b>NOT</b>	<b>PASS 1</b>

quantum yield ( $\Phi_F(\text{Trp})$ ) and lifetime ( $\tau_{\text{Trp}}$ ) as outputs, then two new logic gates can be implemented (see Figure 3). If positive logic conventions are adopted for all of the variables involved and the threshold values of 0.7 for the ratio  $n_{\text{FL}}/n_{\text{Trp}}$ , 0.08 for  $\Phi_F(\text{Trp})$  and 1.5 ns for  $\tau_{\text{Trp}}$  are fixed, then a NOT logic gate, based on  $\Phi_F(\text{Trp})$ , and a PASS 1 based on  $\tau_{\text{Trp}}$ , can be defined (see Table 3). Their speed of computation is of the order of gigahertz.

Whereas the interplay between BSA and FL has mutual effects, that between Trp and FL exerts effects just on Trp fluorescence. In fact, the fluorescence quantum yield ( $\Phi_F(\text{FL})$ ) and lifetime ( $\tau_{\text{FL}}$ ) of FL are insensitive to Trp. Therefore, two PASS 0 logic gates can be defined, having the molar ratio  $n_{\text{Trp}}/n_{\text{FL}}$  as inputs,  $\Phi_F(\text{FL})$  and  $\tau_{\text{FL}}$  as outputs (see Table 4) and a speed of computation of the order of gigahertz.

**3.2. Fuzzy Logic Gates.** It is known that the fluorescence quantum yield of Trp<sup>9</sup> and of proteins having Trp in their backbone<sup>10</sup> can be modulated through an external physical parameter such as the temperature. In the absence of any chemical quencher, the main relaxation paths of the excited Trp are radiative and intersystem crossing routes besides photoionization and intramolecular proton transfer processes. The last

**TABLE 4: Truth Tables for Two PASS 0 Logic Gates Based on FL Photophysics Unaffected by Addition of Trp**

INPUT	OUTPUTS	
$n_{\text{Trp}}/n_{\text{FL}}$	$\Phi_F(\text{FL})$	$\tau_{\text{FL}}$
0 (low) < 5	0 (low) < 0.006	0 (short) < 2 ns
1 (high) > 5	0 (low) < 0.006	0 (short) < 2 ns
	<b>PASS 0</b>	<b>PASS 0</b>

two chemical transformations are thermally activated. Therefore, by increasing the temperature, the energy barrier to nonradiative decay channels can be more easily overcome and the emissive power of Trp weakens. This effect is particularly pronounced when Trp is embedded into a protein, because heating triggers further conformational deactivation pathways.

The experimental data, pointing up the dependence of Trp fluorescence on the temperature and the number of FL moles, are shown in Table 5 for Trp bound to BSA, and in Table 6 for the amino acid dissolved in phosphate buffer.

Three-dimensional (3D) graphs depicting the dependence of  $\Phi_F(\text{BSA})$  and  $\Phi_F(\text{Trp})$  on  $T$  and the number of FL moles are shown in Figure 4, parts a and b, respectively.

From a glance at the two 3D graphs, it clearly emerges that there exist smooth transitions from high to low values of fluorescence quantum yields for both BSA and Trp.  $\Phi_F(\text{BSA})$  and  $\Phi_F(\text{Trp})$  are maximized when both inputs,  $T$  and  $n_{\text{FL}}/n_i$  (where  $i$  is BSA or Trp), are low. Moreover,  $\Phi_F(\text{BSA})$  and  $\Phi_F(\text{Trp})$  exhibit not symmetrical responses to  $T$  and  $n_{\text{FL}}/n_i$ . In fact, at least inside the ranges explored, the molar ratio,  $n_{\text{FL}}/n_i$ , has a stronger effect in determining the fluorescence quantum yield than  $T$ , especially in the case of Trp. The slope of  $\Phi_F(\text{BSA})$  vs  $T$  plot presents a maximum at around 300 K, that decreases at high values of  $n_{\text{FL}}/n_i$ . The dependence of  $\Phi_F(\text{Trp})$  on  $T$  is stronger at lower temperatures and is attenuated at high values of  $n_{\text{FL}}/n_i$ . The smooth and not abrupt three-dimensional profiles representing the dependence of  $\Phi_F(\text{BSA})$  and  $\Phi_F(\text{Trp})$  on  $T$  and  $n_{\text{FL}}/n_i$  are not appropriate for the implementation of binary logic gates, but are ideal to process fuzzy logic. This conclusion was also drawn about the computational power of biochemical reaction networks such as those controlling the glycolysis/gluconeogenesis<sup>11</sup> functions. The switching from glycolysis to gluconeogenesis in response to chemical signals of low blood glucose and abundant fuel for the tricarboxylic acid cycle, has a smooth hyperbolic shape and not a steep sigmoidal response;<sup>12</sup> therefore, it is apt to process fuzzy logic. Similarly, the gradual lessening of  $\Phi_F(\text{BSA})$  and  $\Phi_F(\text{Trp})$  under the synergetic action of the two inputs,  $T$  and  $n_{\text{FL}}/n_i$ , is suitable to implement Fuzzy Logic Systems based on the AND operator. The universes of discourse for  $n_{\text{FL}}/n_i$ ,  $T$ , and  $\Phi_F$  are [0 11], [290 310], [0.035 0.12] in the case of BSA and [0 1.5], [293 318], [0.05 0.14] in the case of Trp. Fuzzy Logic Systems (FLSs) can be implemented by the Mamdani's method.<sup>13</sup> First of all, Mamdani's method requires that experts perform the fuzzification of the parameters involved; in other words, they are supposed to partition the variables in fuzzy sets defining their related membership functions ( $\mu$ ). The  $n_{\text{FL}}/n_i$  variable can be decomposed in three fuzzy sets labeled as (1) low, with a membership function ( $\mu_L$ ) defined by an asymmetrical polynomial curve open to the left (whose symbol will be zmf, [1.5 4] for BSA, [0.25 0.5] for Trp), (2) medium, with  $\mu_M$  having triangular shape (whose symbol will be trimf, [1 5.5 10] for BSA, [0.35 0.65 0.9] for Trp), and (3) high, having an asymmetrical polynomial curve open to the right (whose symbol will be smf, [7 10.5] for BSA, [0.8 1.1] for Trp) as membership function ( $\mu_H$ ). The other input variable,  $T$ , can also be decomposed in other three fuzzy

**TABLE 5: Fluorescence Quantum Yield of BSA at Different Temperatures ( $T$ ) and for Different Values of the Molar Ratio  $n_{\text{FL}}/n_{\text{BSA}}^a$** 

$n_{\text{FL}}/n_{\text{BSA}}$	$\Phi_{\text{F}}(\text{BSA})$					
	$T = 293 \text{ K}$	$T = 295 \text{ K}$	$T = 298 \text{ K}$	$T = 301 \text{ K}$	$T = 303 \text{ K}$	$T = 308 \text{ K}$
0	0.106	0.103*	0.100	0.089*	0.077	0.064*
0.52	0.099*	0.100	0.093*	0.086	0.072*	0.062
1.05	0.095	0.095*	0.091	0.081*	0.069	0.058*
1.57	0.093*	0.089	0.085*	0.077	0.066*	0.055
2.09	0.088	0.087*	0.082	0.076*	0.063	0.054*
2.62	0.085*	0.084	0.080*	0.072	0.060*	0.053
3.14	0.081	0.082*	0.078	0.071*	0.058	0.051*
3.66	0.075*	0.079	0.075*	0.069	0.057*	0.049
4.19	0.072	0.077*	0.070	0.068*	0.054	0.048*
4.71	0.070*	0.074	0.068*	0.066	0.053*	0.046
5.25	0.068	0.072*	0.064	0.065*	0.052	0.046*
5.76	0.065*	0.068	0.061*	0.062	0.050*	0.045
6.28	0.062	0.065*	0.060	0.061*	0.048	0.044*
6.8	0.060*	0.063	0.058*	0.058	0.048*	0.043
7.33	0.059	0.062*	0.054	0.056*	0.047	0.042*
7.87	0.056*	0.061	0.053*	0.054	0.046*	0.042
8.36	0.054	0.059*	0.053	0.053*	0.045	0.041*
8.89	0.053*	0.058	0.050*	0.052	0.044*	0.041
9.43	0.0509	0.0557*	0.0486	0.051*	0.043	0.040*
9.96	0.0494*	0.0538	0.0473*	0.050	0.042*	0.040
10.5	0.0469	0.0536*	0.0460	0.049*	0.040	0.039*

<sup>a</sup> The experimental data are split into training (without asterisk) and checking data (with an asterisk) for the implementation of a Fuzzy Logic System based on the Sugeno's method (see text below).

**TABLE 6: Fluorescence Quantum Yield of Trp at Different Temperatures ( $T$ ) and for Different Values of the Molar Ratio  $n_{\text{FL}}/n_{\text{Trp}}^a$** 

$n_{\text{FL}}/n_{\text{Trp}}$	$\Phi_{\text{F}}(\text{Trp})$					
	$T = 296 \text{ K}$	$T = 299 \text{ K}$	$T = 303 \text{ K}$	$T = 305.5 \text{ K}$	$T = 309 \text{ K}$	$T = 313.3 \text{ K}$
0	0.130	0.120*	0.110	0.105*	0.096	0.085*
0.063	0.126*	0.116	0.106*	0.100	0.095*	0.083
0.126	0.122	0.114*	0.102	0.097*	0.091	0.082*
0.189	0.118*	0.109	0.099*	0.093	0.087*	0.078
0.252	0.114	0.104*	0.094	0.088*	0.085	0.076*
0.315	0.111*	0.102	0.091*	0.085	0.083*	0.074
0.377	0.105	0.098*	0.090	0.082*	0.079	0.072*
0.440	0.103*	0.095	0.086*	0.080	0.076*	0.069
0.503	0.101	0.092*	0.083	0.078*	0.076	0.067*
0.566	0.097*	0.089	0.080*	0.075	0.072*	0.065
0.629	0.095	0.088*	0.078	0.071*	0.071	0.063*
0.692	0.094*	0.085	0.075*	0.070	0.069*	0.061
0.755	0.090	0.083*	0.072	0.067*	0.067	0.059*
0.818	0.086*	0.079	0.070*	0.065	0.064*	0.057
0.881	0.085	0.077*	0.068	0.063*	0.062	
0.944	0.084*	0.074	0.066*	0.060	0.059*	
1.007	0.081	0.073*	0.064	0.059*	0.058	
1.070	0.080*	0.071	0.062*	0.057		
1.133	0.077	0.069*	0.061	0.055*		
1.196	0.074*					
1.259	0.071					

<sup>a</sup> The experimental data are split into training (without asterisk) and checking data (with an asterisk) for the implementation of a Fuzzy Logic System based on the Sugeno's method (see text below).

sets: (1) low (with a zmf  $\mu_{\text{L}}$ , [293 298] for BSA, [296 301] for Trp); (2) medium (with a trmf  $\mu_{\text{M}}$ , [295 300 305] for BSA, [295.5 303.5 310] for Trp); (3) high (with a smf  $\mu_{\text{H}}$ , [301 308] for BSA, [305 313] for Trp). Also the output variable,  $\Phi_{\text{F}}$ , can be split in three fuzzy sets: (1) low (with a zmf  $\mu_{\text{L}}$ , [0.042 0.065] for BSA, [0.07 0.095] for Trp); (2) medium (with a trmf  $\mu_{\text{M}}$ , [0.05 0.074 0.095] for BSA, [0.07 0.093 0.12] for Trp) and (3) high (with a smf  $\mu_{\text{H}}$ , [0.085 0.1] for BSA, [0.105 0.12] for Trp). A representation of the fuzzy sets for all the variables involved is portrayed in Figure 5.

The next step required to implement Mamdani's FLSs entails formulating fuzzy rules. Fuzzy rules are IF-THEN statements,

wherein the IF-part is called the antecedent, and the THEN-part is called the consequence. In our case, due to the synergetic action of the inputs, the dual antecedents are connected through the AND operator. Some representative experimental data of  $T$ ,  $n_{\text{FL}}/n_{\text{i}}$ , and  $\Phi_{\text{F}}$  can be used to infer the fuzzy rules, as in the following examples:

(R<sup>1,1</sup>): IF  $n_{\text{FL}}/n_{\text{i}}$  is low AND  $T$  is low, THEN  $\Phi_{\text{F}}$  is high;

(R<sup>2,3</sup>): IF  $n_{\text{FL}}/n_{\text{i}}$  is medium AND  $T$  is high, THEN  $\Phi_{\text{F}}$  is low.

The entire collection of fuzzy rules, involving the AND connective, is summarized in a matrix (Table 7). It is valid for both BSA and Trp and it consists of nine rules.

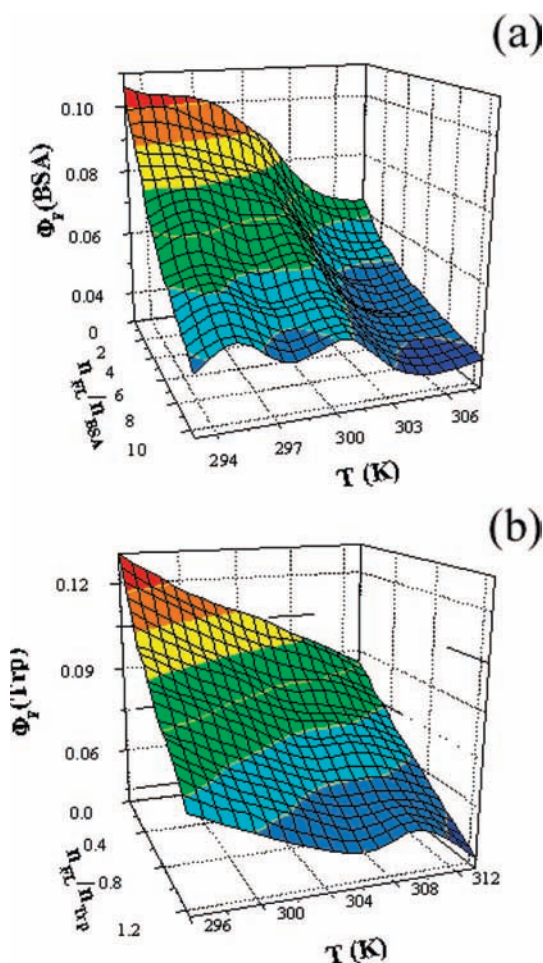


**Figure 4.** Three-dimensional representations of the dependence of fluorescence quantum yield of (a) BSA ( $\Phi_F(\text{BSA})$ ) on temperature ( $T$ ) and molar ratio  $n_{\text{FL}}/n_{\text{BSA}}$ , and of (b)  $\Phi_F(\text{Trp})$  on  $T$  and the molar ratio  $n_{\text{FL}}/n_{\text{Trp}}$ .

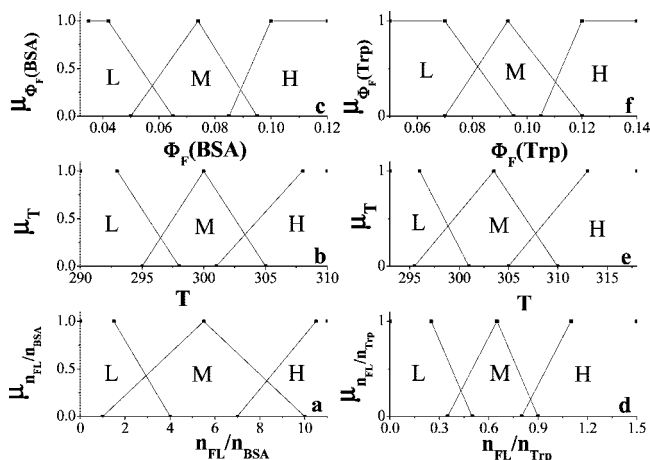


**Figure 5.** Partitions of input and output variables  $n_{\text{FL}}/n_i$ ,  $T$ ,  $\Phi_F$  in fuzzy sets labeled low (L), medium (M), and high (H), in the case of BSA (a,b,c) and Trp (d,e,f). The ordinates represent the membership function values for the different fuzzy sets.

As soon as the fuzzy rules are fixed, the fuzzy inference engine has to be defined and started up. Each rule is interpreted as a fuzzy implication and its membership function is defined through the minimum  $t$ -norm operator.<sup>14</sup> Moreover, the IF–THEN rules are connected through the fuzzy union, i.e.,  $t$ -conorm operator, that means finding the maximum value for the membership functions of the rules involved. The last element

**TABLE 7: Rule Matrix for the FLSs Built upon the Dependence of  $\Phi_F$  on  $n_{\text{FL}}/n_i$  and  $T$  for both BSA and Trp**

$n_{\text{FL}}/n_i$		$T$	
(1) L	$H$	$M$	$M$
(2) M	$M$	$M$	$L$
(3) H	$L$	$L$	$L$
	(1) L	(2) M	(3) H

of the FLS is the defuzzifier whose choice can be ultimately made in the attempt of optimizing the prediction capabilities of each FLS. The FLSs built so far through the Mamdani's approach, are coarse representations of the phenomena on which are based, since they involve a limited number of fuzzy sets.

To give rise to FLSs that are close-fitting descriptions of the experimental evidence, it is useful to adopt the Sugeno's method combined with a neural adaptive learning technique. Sugeno's model<sup>15</sup> entails rules wherein the output membership functions are either constant ( $p_{(j,k)}=q_{(j,k)}=0$ ) or in linear relationship with the inputs (see eq 1):

$$R^{(j,k)} \text{IF } n_{\text{FL}}/n_i \text{ is } F^j(n_{\text{FL}}/n_i) \text{ AND } T \text{ is } F^k(T),$$

$$\text{THEN } \Phi_F = p_{(j,k)} F^j(n_{\text{FL}}/n_i) + q_{(j,k)} F^k(T) + c_{(j,k)} \quad (1)$$

Neural adaptive fuzzy inference systems<sup>16</sup> allow the membership functions to the input/output data to be tailored. Therefore, maintaining the partition of the input spaces,  $n_{\text{FL}}/n_i$  and  $T$ , in three fuzzy sets, adopting bell-shaped membership functions, through a backpropagation-least-squares-based neuro-fuzzy method, nine ( $3 \times 3$ ) rules are generated wherein the consequent parameters  $p_{(j,k)}$ ,  $q_{(j,k)}$ , and  $c_{(j,k)}$  are fixed by the training data of Tables 5 and 6. The structure of the resulting adaptive neuro-fuzzy inference system is portrayed in Figure 6.

The so-built Sugeno's FLSs have strong prediction capabilities. In fact, the checking data of Tables 5 and 6 can be accurately predicted within the accuracy they have been experimentally determined.

#### 4. Conclusions

Molecular computing hinges on intramolecular and intermolecular forces. This work highlights how the intermolecular forces established between FL and BSA or Trp allow us to process logic functions. The photophysics of BSA and Trp are remarkably influenced by the presence of FL molecules,

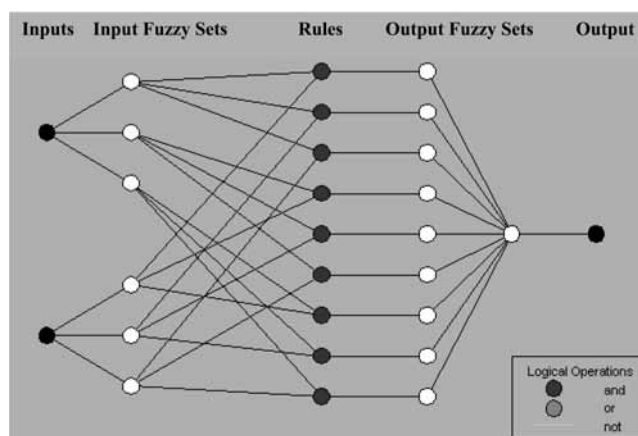


**Figure 6.** Schematic structure of the adaptive neuro-fuzzy inference systems built upon the dependence of BSA and Trp fluorescence quantum yield on  $T$  and the molar ratio  $n_{\text{FL}}/n_i$  through the Sugeno's method.

whereby specific Boolean logic gates can be implemented. Moreover, the structurally more complex BSA exerts appreciable effects also on FL photoresponse, allowing richer logic functions to be treated than in the case of Trp/FL couple.

The relaxation dynamics of BSA and Trp after photoexcitation can be altered not only by addition of FL molecules but also by a physical parameter such as the temperature. Since the relations between the output, fluorescence quantum yield of BSA or Trp, and the inputs,  $n_{FL}/n_i$  and  $T$ , are smooth and not sigmoidal, they are ideal to process fuzzy logic. The synergetic action of the two inputs allows the AND fuzzy logic gate to be implemented, as it has been previously inferred in the case of the proximity effect, wherein the fluorescence quantum yield of FL can be continuously reduced by increasing two physical inputs, such as the temperature and the hydrogen bonding donation ability of the surrounding solvent.<sup>6</sup>

Finally, this work confirms that the Sugeno's method, combined with a neural adaptive learning technique, guarantees the definition of FLSs that are tighter representation of the phenomenon upon which they are built.

Although there is still much work to do before realizing the first binary and fuzzy chemical computers, the molecular logic devices put forward here and elsewhere can find ready application as probes, sensors, and control systems. However, in order to propose probes that can be useful also in media that absorb large portions of the UV spectral region, it would be worthwhile to find molecular processors consisting of dyes that can emit in the visible and near-infrared regions. Molecules emitting visible light signals can establish a link between the macroscopic and the microscopic worlds, making feasible human–molecule communication.

**Acknowledgment.** I thank Prof. Gianna Favaro for her valuable comments on the manuscript. This research was funded by the Italian “Ministero per l'Università e la Ricerca Scientifica e Tecnologica” and the University of Perugia in the framework of a PRIN-2006 Project. (Photophysics and photochemistry of chromogenic compounds for technological applications.)

## References and Notes

- (1) (a) de Silva, A. P.; McClenaghan, N. D. *Chem. Eur. J.* **2004**, *10*, 574–586. (b) Ballardini, R.; Ceroni, P.; Credi, A.; Gandolfi, M. T.; Maestri, M.; Semararo, M.; Venturi, M.; Balzani, V. *Adv. Funct. Mater.* **2007**, *17*, 740–750. (c) Raymo, F. M. *Adv. Funct. Mater.* **2002**, *14*, 401–414, and references therein.
- (2) Wilson, E. K. *Chem. Eng. News* **2000**, *78*, 35–39.
- (3) Ball, P. *Nature* **2000**, *406*, 118–120, and references therein.
- (4) Zadeh, L. A. *IEEE Software* **1994**, *11*, 48–56.
- (5) Deaton, R.; Garzon, M. *Soft Computing* **2001**, *5*, 2–9.
- (6) Gentili, P. L. *Chem. Phys.* **2007**, *336*, 64–73.
- (7) Gentili, P. L.; Ortica, F.; Favaro, G. J. *Phys. Chem. B*, submitted for publication.
- (8) Natick, M. A. *Math Works* 1995.
- (9) Robbins, R. J.; Fleming, G. R.; Beddard, G. S.; Robinson, G. W.; Thistlethwaite, P. J.; Woolfe, G. J. *J. Am. Chem. Soc.* **1980**, *102*, 6271–6279.
- (10) Laustriat, G.; Gerard, G. In *Excited States of Biological Molecules*; Birks, J. B., Ed.; John Wiley and Sons Ltd.: New York, 1976; pp 388–399.
- (11) Arkin, A.; Ross, J. *Biophys. J.* **1994**, *67*, 560–578.
- (12) Bray, D. *Nature* **1995**, *376*, 307–312.
- (13) (a) Mamdani, E. H.; Assilian, S. *Proc. Inst. Elect. Eng.* **1974**, *121*, 1585–1588. (b) Mamdani, E. H.; Assilian, S. *Int. J. Man-Mach. Studies* **1975**, *7*, 1–13.
- (14) Mendel, J. *Proc. IEEE* **1995**, *83*, 345–377.
- (15) Sugeno, M.; Yasukhiro, T. *IEEE Trans. Fuzzy Syst.* **1993**, *1*, 7–31.
- (16) (a) Jang, J. S. R.; Sun, C. T. *Proc. IEEE* **1995**, *83*, 378–405. (b) Jang, J. S. R. *IEEE Trans. Syst., Man Cybern.* **1993**, *23*, 665–684.

JP806772M